

AperTO - Archivio Istituzionale Open Access dell'Università di Torino

## Diamond detector technology, status and perspectives

### This is the author's manuscript

*Original Citation:*

*Availability:*

This version is available <http://hdl.handle.net/2318/1675878> since 2019-04-05T09:28:03Z

*Published version:*

DOI:10.1016/j.nima.2018.06.009

*Terms of use:*

Open Access

Anyone can freely access the full text of works made available as "Open Access". Works made available under a Creative Commons license can be used according to the terms and conditions of said license. Use of all other works requires consent of the right holder (author or publisher) if not exempted from copyright protection by the applicable law.

(Article begins on next page)

Manuscript Number:

Title: Diamond detector technology, status and perspectives

Article Type: SI: NIMA-HSTD 2017

Keywords: Chemical Vapor Deposition; pCVD diamond; diamond detectors; 3D diamond detectors; radiation tolerant detectors

Corresponding Author: Professor Harris Kagan, Ph.D.

Corresponding Author's Institution: Ohio State University

First Author: Harris Kagan, Ph.D.

Order of Authors: Harris Kagan, Ph.D.; A. Alexopoulos; M. Artuso; F. Bachmair; L. Baeni; M. Bartosik; J. Beacham; H. Beck; V. Bellini; V. Belyaev; B. Bentele; P. Bergonzo; A. Bes; J-M. Brom; M. Bruzzi; G. Chiodini; D. Chren; V. Cindro; G. Claus; J. Collot; J. Cumalat; A. Dabrowski; R. D'Alessandro; D. Dauvergne; W. de Boer; S. Dick; C. Dorfer; M. Dunser; V. Eremin; G. Forcolin; J. Forneris; L. Gallin-Martel; M-L. Gallin-Martel; K.K. Gan; M. Gastal; C. Giroletti; M. Goffe; J. Goldstein; A. Golubev; A. Gorisek; E. Grigoriev; J. Grosse-Knetter; A. Grummer; B. Gui; M. Guthoff; I. Haughton; B. Hiti; D. Hits; M. Hoferkamp; T. Hofmann; J. Hosslet; J-Y. Hostachy; F. Huegging; C. Hutton; J. Janssen; K. Kanxheri; G. Kasieczka; R. Kass; F. Kassel; M. Kis; G. Kramberger; S. Kuleshov; S. Kuleshov; A. Lacoste; S. Lagomarsino; A. Lo Giudice; E. Lukosi; C. Maazouzi; I. Mandic; C. Mathieu; M. Menichelli; M. Mikuz; A. Morozzi; J. Moss; R. Mountain; S. Murphy; M. Muskinja; A. Oh; P. Oliviero; D. Passeri; H. Pernegger; R. Perrino; F. Picollo; M. Pomorski; R. Potenza; A. Quadt; A. Re; M. Reichmann; G. Riley; S. Roe; D. Sanz; M. Scaringella; D. Schaefer; C.J. Schmidt; D.S. Smith; S. Schnetzer; S. Sciortino; A. Scorzoni; S. Seidel; L. Servoli; B. Sopko; V. Sopko; S. Spagnolo; S. Spanier; K. Stenson; R. Stone; C. Sutura; A. Taylor; B. Tannenwald; M. Traeger; D. Tromson; W. Trischuk; C. Tuve; J. Velthuis; N. Venturi; E. Vittone; S. Wagner; R. Wallny; J.C. Wang; J. Weingarten; C. Weiss; T. Wengler; N. Wermes; M. Yamouni; M. Zavrtnik

Abstract: Detectors based on Chemical Vapor Deposition (CVD) diamond have been used extensively and successfully in beam conditions/beam loss monitors as the innermost detectors in the highest radiation areas of Large Hadron Collider (LHC) experiments. The startup of the LHC in 2015 brought a new milestone where the first polycrystalline CVD (pCVD) diamond pixel modules were installed in an LHC experiment and successfully began operation. The RD42 collaboration at CERN is leading the effort to develop polycrystalline CVD diamond as a material for tracking detectors operating in extreme radiation environments. The status of the RD42 project with emphasis on recent beam test results is presented.

## Diamond detector technology, status and perspectives

2 H. Kagan<sup>m</sup>, A. Alexopoulos<sup>c</sup>, M. Artuso<sup>l</sup>, F. Bachmair<sup>x</sup>, L. Bäni<sup>x</sup>, M. Bartosik<sup>c</sup>, J. Beacham<sup>m</sup>,  
 3 H. Beck<sup>w</sup>, V. Bellini<sup>b</sup>, V. Belyaev<sup>l</sup>, B. Bentele<sup>s</sup>, P. Bergonzo<sup>k</sup>, A. Bes<sup>aa</sup>, J-M. Brom<sup>g</sup>,  
 4 M. Bruzzi<sup>d</sup>, G. Chiodini<sup>z</sup>, D. Chren<sup>r</sup>, V. Cindro<sup>j</sup>, G. Claus<sup>g</sup>, J. Collot<sup>aa</sup>, J. Cumalat<sup>s</sup>,  
 5 A. Dabrowski<sup>c</sup>, R. D'Alessandro<sup>d</sup>, D. Dauvergne<sup>aa</sup>, W. de Boer<sup>j</sup>, S. Dick<sup>m</sup>, C. Dorfer<sup>x</sup>,  
 6 M. Dunser<sup>c</sup>, V. Eremin<sup>f</sup>, G. Forcolin<sup>v</sup>, J. Forneris<sup>o</sup>, L. Gallin-Martel<sup>aa</sup>, M-L. Gallin-Martel<sup>aa</sup>,  
 7 K.K. Gan<sup>m</sup>, M. Gastal<sup>c</sup>, C. Giroletti<sup>q</sup>, M. Goffe<sup>g</sup>, J. Goldstein<sup>q</sup>, A. Golubev<sup>h</sup>, A. Gorišek<sup>i</sup>,  
 8 E. Grigoriev<sup>h</sup>, J. Grosse-Knetter<sup>w</sup>, A. Grummer<sup>u</sup>, B. Gui<sup>m</sup>, M. Guthoff<sup>c</sup>, I. Haughton<sup>v</sup>,  
 9 B. Hiti<sup>i</sup>, D. Hits<sup>x</sup>, M. Hoferkamp<sup>u</sup>, T. Hofmann<sup>c</sup>, J. Hosslet<sup>g</sup>, J-Y. Hostachy<sup>aa</sup>, F. Hügging<sup>a</sup>,  
 10 C. Hutton<sup>q</sup>, J. Janssen<sup>a</sup>, K. Kanxheri<sup>ab</sup>, G. Kasieczka<sup>x</sup>, R. Kass<sup>m</sup>, F. Kassel<sup>j</sup>, M. Kis<sup>c</sup>,  
 11 G. Kramberger<sup>i</sup>, S. Kuleshov<sup>h</sup>, A. Lacoste<sup>aa</sup>, S. Lagomarsino<sup>d</sup>, A. Lo Giudice<sup>o</sup>, E. Lukosi<sup>v</sup>,  
 12 C. Maazouzi<sup>g</sup>, I. Mandic<sup>i</sup>, C. Mathieu<sup>g</sup>, M. Menichelli<sup>ab</sup>, M. Mikuž<sup>i</sup>, A. Morozzi<sup>ab</sup>,  
 13 J. Moss<sup>ac</sup>, R. Mountain<sup>l</sup>, S. Murphy<sup>v</sup>, M. Muškinja<sup>i</sup>, A. Oh<sup>v</sup>, P. Oliviero<sup>o</sup>, D. Passeri<sup>ab</sup>,  
 14 H. Pernegger<sup>c</sup>, R. Perrino<sup>z</sup>, F. Picollo<sup>o</sup>, M. Pomorski<sup>k</sup>, R. Potenza<sup>b</sup>, A. Quadt<sup>w</sup>, A. Re<sup>o</sup>,  
 15 M. Reichmann<sup>x</sup>, G. Riley<sup>v</sup>, S. Roe<sup>c</sup>, D. Sanz<sup>x</sup>, M. Scaringella<sup>d</sup>, D. Schaefer<sup>c</sup>, C.J. Schmidt<sup>e</sup>,  
 16 D.S. Smith<sup>m</sup>, S. Schnetzer<sup>n</sup>, S. Sciortino<sup>d</sup>, A. Scorzoni<sup>ab</sup>, S. Seidel<sup>u</sup>, L. Servoli<sup>ab</sup>, B. Sopko<sup>r</sup>,  
 17 V. Sopko<sup>r</sup>, S. Spagnolo<sup>z</sup>, S. Spanier<sup>v</sup>, K. Stenson<sup>s</sup>, R. Stone<sup>n</sup>, C. Sutura<sup>b</sup>, A. Taylor<sup>u</sup>,  
 18 B. Tannenwald<sup>m</sup>, M. Traeger<sup>e</sup>, D. Tromson<sup>k</sup>, W. Trischuk<sup>p</sup>, C. Tuve<sup>b</sup>, J. Velthuis<sup>q</sup>,  
 19 N. Venturi<sup>c</sup>, E. Vittone<sup>o</sup>, S. Wagner<sup>s</sup>, R. Wallny<sup>x</sup>, J.C. Wang<sup>t</sup>, J. Weingarten<sup>w</sup>, C. Weiss<sup>c</sup>,  
 20 T. Wengler<sup>c</sup>, N. Wermes<sup>a</sup>, M. Yamouni<sup>aa</sup>, M. Zavrtanik<sup>i</sup>

<sup>a</sup>Universität Bonn, Bonn, Germany

<sup>b</sup>INFN/University of Catania, Catania, Italy

<sup>c</sup>CERN, Geneva, Switzerland

<sup>d</sup>INFN/University of Florence, Florence, Italy

<sup>e</sup>GSI, Darmstadt, Germany

<sup>f</sup>Ioffe Institute, St. Petersburg, Russia

<sup>g</sup>IPHC, Strasbourg, France

<sup>h</sup>ITEP, Moscow, Russia

<sup>i</sup>Jozef Stefan Institute, Ljubljana, Slovenia

<sup>j</sup>Universität Karlsruhe, Karlsruhe, Germany

<sup>k</sup>CEA-LIST Technologies Avancees, Saclay, France

<sup>l</sup>MEPHI Institute, Moscow, Russia

<sup>m</sup>The Ohio State University, Columbus, OH, USA

<sup>n</sup>Rutgers University, Piscataway, NJ, USA

<sup>o</sup>University of Torino, Torino, Italy

<sup>p</sup>University of Toronto, Toronto, ON, Canada

<sup>q</sup>University of Bristol, Bristol, UK

<sup>r</sup>Czech Technical Univ., Prague, Czech Republic

<sup>s</sup>University of Colorado, Boulder, CO, USA

<sup>t</sup>Syracuse University, Syracuse, NY, USA

<sup>u</sup>University of New Mexico, Albuquerque, NM, USA

<sup>v</sup>University of Manchester, Manchester, UK

<sup>w</sup>Universität Goettingen, Goettingen, Germany

<sup>x</sup>ETH Zürich, Zürich, Switzerland

<sup>y</sup>University of Tennessee, Knoxville, TN, USA

<sup>z</sup>INFN-Lecce, Lecce, Italy

<sup>aa</sup>LPSC-Grenoble, Grenoble, France

<sup>ab</sup>INFN-Perugia, Perugia, Italy

<sup>ac</sup>California State University, Sacramento, CA, USA

---

50 **Abstract**

51 Detectors based on Chemical Vapor Deposition (CVD) diamond have been used extensively  
52 and successfully in beam conditions/beam loss monitors as the innermost detectors in the highest  
53 radiation areas of Large Hadron Collider (LHC) experiments. The startup of the LHC in 2015  
54 brought a new milestone where the first polycrystalline CVD (pCVD) diamond pixel modules  
55 were installed in an LHC experiment and successfully began operation. The RD42 collaboration  
56 at CERN is leading the effort to develop polycrystalline CVD diamond as a material for tracking  
57 detectors operating in extreme radiation environments. The status of the RD42 project with  
58 emphasis on recent beam test results is presented.

59 *Keywords:* Chemical Vapor Deposition, pCVD diamond, diamond detectors, 3D diamond  
60 detectors, radiation tolerant detectors

---

61 **1. Introduction**

62 The RD42 collaboration [1, 2] at CERN is leading the effort to develop radiation tolerant  
63 devices based on pCVD diamond as a material for tracking detectors operating in harsh radiation  
64 environments. Diamond has properties which make it suitable for such detector applications.  
65 During the last few years the RD42 group has succeeded in producing and measuring a number  
66 of devices to address specific issues related to use at the HL-LHC [3, 4]. This paper presents  
67 the status of the RD42 project with emphasis on recent beam test results. In particular, results  
68 are presented on the status of the first diamond pixel detector based on pCVD material, on the  
69 independence of signal size on incident particle rate in pCVD diamond detectors over a range of  
70 particle fluxes up to 20 MHz/cm<sup>2</sup> and on the 3D diamond detectors fabricated in pCVD diamond.

71 **2. Status of the ATLAS Diamond Beam Monitor**

72 The startup of the LHC in 2015 brought a new milestone for diamond detector development  
73 where the first planar diamond pixel modules based on pCVD diamond were installed in an  
74 LHC experiment, the ATLAS experiment [5], and successfully began operation. The ATLAS  
75 Diamond Beam Monitor (DBM) [6, 7] was designed to measure the instantaneous luminosity,  
76 the background rates and the beam spot position. A single DBM module consists of an 18 mm ×  
77 21 mm pCVD diamond 500 μm thick instrumented with a FE-I4 pixel chip [8]. The 26,880 pixels  
78 are arranged in 80 columns on 250 μm pitch and 336 rows on 50 μm pitch resulting in an active  
79 area of 16.8 mm × 20.0 mm. This fine granularity provides high precision particle tracking. The  
80 deposited charge from a particle is measured in the FE-I4 by Time-over-Threshold.

81 The ATLAS DBM uses diamonds with a charge collection distance (the average distance an  
82 electron-hole pair move apart under the influence of the applied electric field) of 200-220 μm at  
83 an applied bias voltage of 500 V. Three telescopes each with 3 diamond DBM modules (plus 1  
84 telescope with silicon sensors) mounted as a three layer tracking device were installed inside the  
85 pixel detector services on each side of the ATLAS interaction point at 90 cm < |z| < 111 cm,

---

*Email address:* harris.kagan@cern.ch (H. Kagan)

86  $3.2 < |\eta| < 3.5$  and at a radial distance from 5 cm to 7 cm from the center of the beam pipe. The  
 87 modules have an inclination of  $10^\circ$  with respect to the ATLAS solenoid magnetic field direction  
 88 to suppress erratic dark currents [9] in the diamonds. The ATLAS DBM data-acquisition system  
 89 is shared with the ATLAS IBL [10]. After initial installment, data were collected in the July 2015  
 90 run. These data have been analyzed and the first results of the ATLAS DBM tracking capabilities  
 91 are shown in Fig. 1. A clear separation between background particles from unpaired bunches  
 92 (open circles) and collision particles from colliding bunches (filled circles) is observed. After  
 93 two electrical incidents in 2015 with consequent loss of several silicon and diamond modules,  
 94 the DBM has now been re-commissioned and is again in the operation phase.

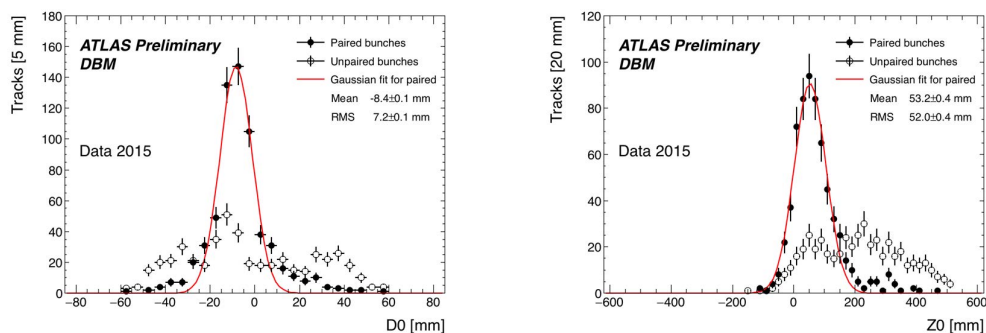


Figure 1: Radial distance (left plot) and longitudinal distance (right plot) of the closest approach of the projected particle tracks to the interaction point as recorded by a single DBM telescope with preliminary alignment.

### 95 3. Rate Studies in pCVD diamond

96 In order to study the dependence of signal size on incident particle rate, RD42 performed a  
 97 series of beam tests in the  $\pi$ M1 beam line of the High Intensity Proton Accelerator (HIPA) at  
 98 Paul Scherrer Institute (PSI) [11]. This beam line is able to deliver 260 MeV/c  $\pi^+$  fluxes from a  
 99 rate of  $\sim 5$  kHz/cm<sup>2</sup> to a rate  $\sim 20$  MHz/cm<sup>2</sup> in bunches spaced 19.8 ns apart.

100 Sensors using pCVD material [12] were tested in a tracking telescope [13] based on  $100 \mu\text{m}$   
 101  $\times 150 \mu\text{m}$  silicon pixel sensors read out by the PSI46v2 pixel chip [14]. The diamond signals  
 102 were amplified with custom-built front-end electronics with a peaking time of  $\sim 6$  ns, return-  
 103 to-baseline in  $\sim 16$  ns and 550e noise with 2 pf input capacitance. The amplified signals were  
 104 recorded with a DRS4 evaluation board [15] operating at 2 GS/s. The entire system was triggered  
 105 with a scintillator which determined the timing of the beam particles with a precision of  $\sim 0.7$  ns.

106 A series of cuts were applied to the data including: removing 60s of seconds of triggers  
 107 at the beginning of each run, removing triggers from heavily ionizing particles with saturated  
 108 waveforms (mostly protons), removing calibration triggers, removing triggers in the wrong beam  
 109 bucket, removing triggers with no tracks in the telescope and removing triggers with large angle  
 110 tracks in the telescope. After applying this procedure all telescope tracks which project into the  
 111 diamond fiducial region have a pulse height well separated from the pedestal distribution in the  
 112 diamond i.e. the diamond is 100% efficient at all rates. The same procedure was applied to all  
 113 particle flux points and the resulting mean pulse height (in arbitrary units) versus rate is shown  
 114 in Fig. 2 for both positive and negative bias voltage. The uncertainty on the data points in the  
 115 plot include both statistical and systematic sources. The systematic uncertainty was determined  
 116 by assuming any deviations in pulse height for rates below 80 kHz/cm<sup>2</sup> was due to systematic

117 effects. Thus the spread in the data points at a given rate indicates the reproducibility of the data.  
 118 Fig. 2 indicates the mean pulse height in pCVD diamond detectors irradiated up to  $5 \times 10^{14}$  n/cm<sup>2</sup>  
 119 does not depend strongly on rate up to rates of 20 MHz/cm<sup>2</sup>.

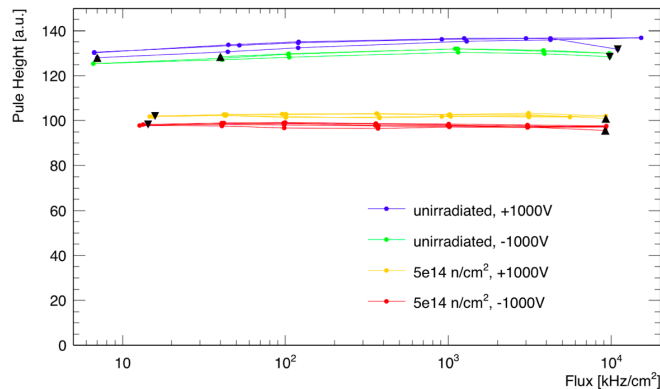


Figure 2: The average pulse height versus rate for an un-irradiated and irradiated pCVD diamond pad detector at positive and negative bias. The beam line parameters were adjusted to set the different particle rates. The data was taken by scanning up and down in rate multiple times. The pulse height units are arbitrary since the un-irradiated and irradiated detectors used different readout electronics. The resulting electronics gain corrections and the relative gain correction for positive versus negative signals in the electronics is still being determined and has not been applied.

#### 120 4. 3D Diamond Pixel Detectors

121 3D sensors with electrodes in the bulk of the sensor material were first proposed in 1997 [16]  
 122 in order to reduce the drift distance of the charged carriers to much less than the sensor thickness.  
 123 In order to achieve this goal a series of alternating + and – electrodes perpendicular to the read  
 124 out face were created in the bulk detector material. This idea is particularly beneficial in detectors  
 125 with a limited mean free path such as trap dominated sensor materials like heavily irradiated  
 126 silicon and pCVD diamond where the observed signal size is related to the mean free path divided  
 127 by the drift distance. Under these circumstances one gains radiation tolerance (larger signals) by  
 128 keeping the drift distance less than the mean free path. With this geometrical structure charge  
 129 carriers drift inside the bulk parallel to the surface over a typical drift distance of 25-100  $\mu$ m  
 130 instead of perpendicular to the surface over a distance of 250-500  $\mu$ m.

131 In 2015 RD42 published results of a 3D device fabricated in single-crystal CVD diamond [17]  
 132 showing that the 3D structure works in diamond. In 2016 RD42 fabricated the first 3D device in  
 133 pCVD diamond [18]. The electrodes in the bulk of the pCVD diamond 3D device were fabricated  
 134 with lasers as described in [17]. The bias electrodes were placed at the corners and the readout  
 135 electrodes were placed in the middle of the cells. This pCVD device was shown to collect more  
 136 than 75% of the deposited charge which translates in more than a factor of two more charge than  
 137 a planar diamond strip detector fabricated on the same pCVD diamond.

138 In 2017 RD42 successfully constructed the first pCVD diamond 3D pixel detector with 50 $\mu$ m  
 139  $\times$  50  $\mu$ m cells. This pixel device is designed to be read out with the RD53 pixel readout chip [19]  
 140 which is not yet available. In order to read this device out with an existing pixel readout chip a  
 141 small number of cells were ganged together to match the pitch of the pixel readout chip. RD42  
 142 is proceeding to make 3D diamond pixel devices compatible with both the CMS pixel readout

143 chip ( $3 \times 2$  ganging) and the ATLAS pixel readout chip ( $1 \times 5$  ganging). The first  $50 \mu\text{m} \times 50$   
 144  $\mu\text{m}$  pCVD diamond 3D pixel device which was bump-bonded used the CMS pixel readout chip.  
 145 This first diamond 3D pixel device was tested during the Aug 2017 beam test at PSI at a  
 146 single voltage and with rates from  $7 \text{ kHz/cm}^2$  to  $7 \text{ MHz/cm}^2$ . During the initial lab test it was  
 147 discovered that the bump bonding had a small issue on one edge. We decided to take data  
 148 with the device rather than try to repair this small bump bonding issue. Fig. 3(left) shows the  
 149 preliminary efficiency as a function of  $xy$  position for every cell in the device with a  $1500 e$   
 150 pixel threshold. The red box marks the fiducial region used to measure the hit efficiency. The  
 151 blue circle indicates the position of the one non-working pixel cell in the central region of the  
 152 device. Fig. 3(right) shows the hit efficiency in the fiducial region with the  $1500 e$  pixel threshold  
 153 as a function of time for an up-down scan of incident particle rates from  $7 \text{ kHz/cm}^2$  (near time  
 154 (0:00) to  $7 \text{ MHz/cm}^2$  (near time 0:12) and back to  $7 \text{ kHz/cm}^2$  (near time 0:24). The overall  
 155 measured efficiency is  $99.4\%$  and no change in efficiency as a function of rate is observed. The  
 156 corresponding efficiency for a planar silicon CMS pixel detector in this test was  $99.9\%$  with no  
 157 change in efficiency as a function of rate. The slight loss of efficiency ( $0.5\%$ ), assuming it holds  
 158 through the completion of the analysis, is most likely due to charge loss in the column electrodes.  
 159 If this explanation is correct, then this effect can be easily remedied by tilting the detector at a  
 160 small angle with respect to the incident beam.

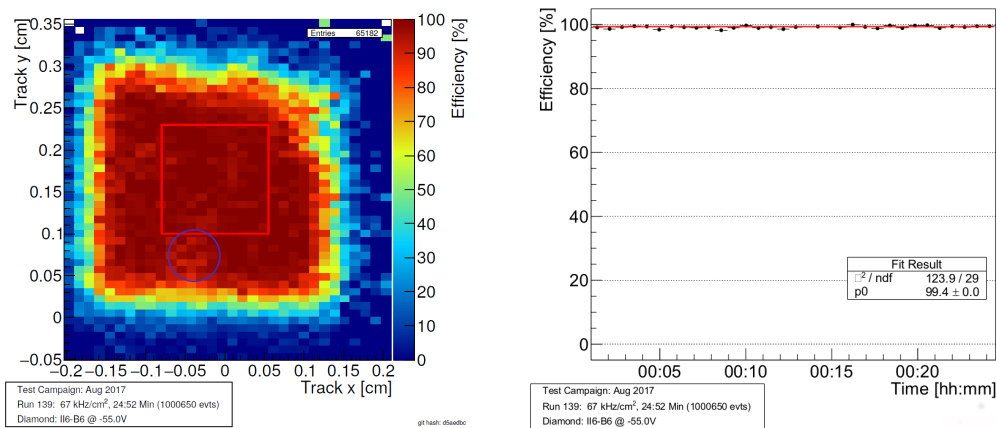


Figure 3: The hit efficiency of the first  $50 \mu\text{m} \times 50 \mu\text{m}$  cell pCVD 3D pixel detector with  $3 \times 2$  ganged cells read out with CMS pixel electronics with a  $1500 e$  threshold. The left plot shows the efficiency of each ganged cell as a function of  $xy$  position in the device. The right plot shows the average efficiency in the fiducial region (the red box in the left plot) as a function of time during a rate scan from  $7 \text{ kHz/cm}^2$  to  $7 \text{ MHz/cm}^2$  and back to  $7 \text{ kHz/cm}^2$ .

## 161 5. Conclusions

162 The recent progress in the design, fabrication and testing of polycrystalline CVD diamond  
 163 detectors was presented. The following milestones have been achieved: successful operation of  
 164 the first pCVD diamond planar pixel detector in the ATLAS experiment at the LHC; demonstra-  
 165 tion that the average signal pulse height of pCVD diamond detectors irradiated up to  $5 \times 10^{14}$   
 166  $\text{n/cm}^2$  is independent of the particle flux up to  $\sim 20 \text{ MHz/cm}^2$ ; successful fabrication and opera-  
 167 tion of the first pCVD diamond 3D pixel detector with  $50 \mu\text{m} \times 50 \mu\text{m}$  pixels read out with CMS  
 168 pixel electronics where the efficiency for a MIP was  $>99\%$  and the average charge collected in  
 169 the device was  $>90\%$  of the deposited charge. In the future RD42 plans to study the pulse height

170 dependence of CVD diamond sensors with pad and pixel electrodes with radiation doses up to  
171  $10^{17}$  n/cm<sup>2</sup> and continue the development of 3D diamond detectors with the production of a 50  
172  $\mu\text{m} \times 50 \mu\text{m}$  cell pCVD diamond 3D pixel detector compatible with ATLAS readout electronics.

## 173 6. Acknowledgments

174 The RD42 Collaboration gratefully acknowledges the staff at CERN for test beam time and  
175 their help in setting up the beam conditions. We would especially like to thank Henric Wilkins,  
176 the test beam coordinator, for his assistance in making our tests a success. We also thank the  
177 beam line staff at the PSI High Intensity Proton Accelerator especially Konrad Deiters, Manuel  
178 Schwarz and Davide Reggiani for their assistance in carrying out the diamond detector tests. We  
179 extend our gratitude to Prof. Lin Li and David Whitehead of the University of Manchester Laser  
180 Processing Center for their assistance in the production of 3D diamond devices. The research  
181 leading to these results received funding from the European Union's Horizon 2020 research and  
182 innovation program under grant agreement No. 654168. This work was also partially supported  
183 by the Swiss National Science Foundation grant #20FL20\_154216, ETH grant 51 15-1, Royal  
184 Society Grant UF120106 and the U.S. Department of Energy through grant DE-SC0010061.

## 185 References

- 186
- 187 [1] W. Adam, *et al.* [RD42 collaboration], *Development of Diamond Tracking Detectors for High Luminosity Experi-*  
188 *ments at the LHC*, Proposal/RD42 CERN/DRDC 94-21, Status Report/RD42, CERN/LHCC, 95-43, 95-53, 95-58,  
189 97-03, 98-20, 2000-011, 2000-015, 2001-002, 2002-010, 2003-063, 2005-003, 2006-010, 2007-002, 2008-005.
  - 190 [2] M. Artuso, *et al.* [RD42 Collaboration], RD42 Status Report: Development of Diamond Tracking Detectors for  
191 High Luminosity Experiments at the LHC, CERN-LHCC-2017-006.
  - 192 [3] G. Apollinari, *et al.*, *Chapter 1: High-Luminosity Large Hadron Collider HL-LHC in High-Luminosity Large*  
193 *Hadron Collider (HL-LHC): Preliminary Design Report*, CERN Yellow Reports: Monographs, CERN-2015-005,  
194 CERN Geneva, 2015, <https://doi.org/10.5170/CERN-2015-005.1>.
  - 195 [4] G. Apollinari, *et al.*, *High-Luminosity Large Hadron Collider (HL-LHC): Technical Design Report*  
196 *V.0.1*, CERN Yellow Reports: Monographs, Volume 4/2017 CERN-2017-007-M, CERN Geneva 2017,  
197 <https://doi.org/10.23731/CYRM-2017-004>.
  - 198 [5] G. Aad, *et al.* [ATLAS collaboration], *The ATLAS experiment at the CERN Large Hadron Collider*, JINST **3**  
199 S08003, 2008.
  - 200 [6] H. Kagan, *et al.*, *ATLAS Diamond Beam Monitor TDR*, ATLAS Document DBM **001** (2011).
  - 201 [7] M. Červ, *et al.*, *The ATLAS Diamond Beam Monitor*, JINST **9** C02026, 2014.
  - 202 [8] M. Barbero, *et al.*, *The FE-14 pixel readout chip and the IBL module*, PoS(Vertex 2011) **038** (2011).
  - 203 [9] A.J. Edwards, *et al.*, *Radiation monitoring with diamond sensors in BABAR*, IEEE Trans. Nucl. Sci. **51** (2004)  
204 1808.
  - 205 [10] F. Huegging, *et al.* [ATLAS Collaboration], *The ATLAS Pixel Insertable B-Layer (IBL)*, Nucl. Instrum. Meth. Phys.  
206 Res. A **650** (2011) 45.
  - 207 [11] PSI High Intensity Proton Accelerator, *High Energy Beam Lines*, <http://www.psi.ch/abe/high-energy-beam-lines>
  - 208 [12] The diamond material for these tests was provided by II-VI Inc., 360 Saxonburg Road, Saxonburg, PA.
  - 209 [13] F. Bachmair, *CVD Diamond Sensors In Detectors For High Energy Physics*, Ph.D. Thesis, ETH Zürich (2016),  
210 <https://doi.org/10.3929/ethz-a-010748643>.
  - 211 [14] H.Chr. Kästli, *et al.*, *Design and performance of the CMS pixel detector readout chip*, Nucl. Instrum. Meth. Phys.  
212 Res. A **565**(2006) 188.
  - 213 [15] S. Ritt, *DRS4 Evaluation Board*, <http://www.psi.ch/drs/evaluation-board>
  - 214 [16] S. Parker, C.J. Kenney and J. Segal, *3-D: A proposed new architecture for solid state radiation detectors*, Nucl.  
215 Instrum. Meth. Phys. Res. A **395** (1997) 328.
  - 216 [17] F. Bachmair, *et al.* [RD42 Collaboration], *A 3D Diamond Detector for Particle Tracking*, Nucl. Instrum. Meth.  
217 Phys. Res. A, **786** (2015) 97.
  - 218 [18] A. Alexopoulos, *et al.* [RD42 Collaboration], *Diamond detector technology: status and perspectives*, PoS(Vertex  
219 2016) **027** 2016.
  - 220 [19] M. Garcia-Sciveres, *et al.* [RD53 Collaboration], *The RD53A Integrated Circuit*, CERN-RD53-PUB-17-001  
221 (2017). <https://cds.cern.ch/record/2287593?ln=en>.